Molecular Mechanics Calculations of 10-Vertex Boron Cage Compounds

Kyrill Yu. Suponitsky[†]

Institute of Organoelement Compounds, Russian Academy of Sciences, Vavilov Street 28, Moscow 117813, Russia

Tatjana V. Timofeeva[‡]

Department of Physical Sciences, New Mexico Highlands University, Las Vegas, New Mexico 87701

Norman L. Allinger*

Computational Center for Molecular Structure and Design, Department of Chemistry, University of Georgia, Athens, Georgia 30602-2556

Received September 29, 1999

The model proposed earlier for molecular mechanics calculations of 7- and 12-vertex boranes, carboranes, and metallocarboranes has been extended to the case of 10-vertex borane cage compounds. To use the MM3 program[1] with the standard connectivity file, and to avoid program alterations, the 10-vertex cages of the molecules were presented as a superposition of four formally independent fragments. Interactions between the fragments were described with a Hill-like potential, with the parameters adjusted for valence interactions. Standard values for the bond lengths and bond angles in the 10-vertex boron cage have been found by statistical analysis of X-ray data on borane cage compounds stored in the Cambridge Structural Database. Several substituted neutral molecules and anions have been considered, and good agreement of the calculated and experimental data has been obtained. Using the approach developed, the unknown structure of the $[\mu\text{-}B_{20}H_{16}O(CH_2)_4O(CH_2)_2CH(CH_3)_2]^{3-}$ ion has been calculated.

Introduction

In our previous publications[2] we have proposed an approach to the calculation of the structures of polyhedral borane compounds by the molecular mechanics (MM) method.[3] The MM3 program[1] has been utilized in these investigations. Boranes, carboranes, and metallocarboranes with 7- and 12-vertex cages have been previously considered, and it has been shown that MM can be successfully used for the investigation and prediction of their structures. Those projects were carried out because the polyhedral borane compounds are an entire class of inorganic compounds with unusual molecular structures and a wide range of properties. It is interesting to note that such properties as the essential stability and benzene-like reactivity of these molecules are associated with their three-dimensional structures. The salts formed by the negatively charged borane cage ions or carborane cage ions are easily dissolved in many electron-donating solvents, and appear to be strong electrolytes. *closo*-Dicarbaboranes are prone to polymer formation.

These properties define potential applications of polyhedral borane compounds, and have been thoroughly discussed, for instance, by Plešek.[4] Here we will mention the most interesting and significant ones, for which MM investigation might be applied. Carboranes may be introduced into polymer chains formed by siloxane fragments, and they increase the thermal stability of such polymers.[5,6] Increased thermal stabilities and refractive indices of liquid crystals can be achieved by involving carboranes as structural elements.[7] Twelve-vertex rhodacarboranes are known to be good homogeneous catalysts.[8] Since polyhedral boranes are nontoxic, they can be used (including some 10-vertex boranes from the present investigation) for the boron neutron capture therapy of tumors.[9]

However, it should be noted that the synthesis of the above-mentioned compounds is difficult and expensive. Therefore, the

* Corresponding author. Fax: (706) 542-2673. E-mail: allinger@sunchem.chem.uga.edu.

[†]Current address: Department of Physical Sciences, New Mexico Highlands University, Las Vegas, NM 87701. Fax: (095) 135-5085. E-mail: kira@kremlin.nmhu.edu.

[‡] Fax: (505) 454-3103. E-mail: tanya@mount.nmhu.edu.

(1) (a) Allinger, N. L.; Yuh, Y. H.; Lii, J.-H. *J. Am. Chem. Soc.* **1989**, *111*, 8551−8566. (b) Lii, J.-H.; Allinger, N. L. *J. Am. Chem. Soc.* **1989**, *111*, 8566−8575. (c) Lii, J.-H.; Allinger, N. L. *J. Am. Chem. Soc.* **1989**, *111*, 8576−8582. (Available to all users from Tripos Associates, 1699 S. Hanley Rd., St. Louis, MO 63144, and to academic users only from the Quantum Chemistry Program Exchange, Indiana University, Bloomington, IN 47405.)

(2) (a) Timofeeva, T. V.; Allinger, N. L.; Buehl, M.; Mazurek, U. *Russ. Chem. Bull.* **1994**, *43*, 1795−1801. (b) Timofeeva, T. V.; Mazurek, U.; Allinger, N. L. *J. Mol. Struct., THEOCHEM* **1996**, *363*, 35−42. (c) Timofeeva, T. V.; Suponitsky, K. Yu.; Yanovsky, A. I.; Allinger, N. L. *J. Organomet. Chem.* **1997**, *536*−*537*, 481−488. (d) Suponitsky, K. Yu.; Timofeeva, T. V.; Chizhevsky, I. T.; Zinevich, T. V.; Allinger, N. L. *Russ. Chem. Bull.* **1998**, *47*, 596−601.

(3) (a) Burkert, U.; Allinger, N. L. *Molecular Mechanics*; American Chemical Society: Washington, DC, 1982. (b) Rappe, A. K.; Casewit, C. J. *Molecular Mechanics Across Chemistry*; University Science Books: Sausalito, CA, 1997.

(4) Plešek, J. *Chem. Rev.* **1992**, *92*, 269−278.

(5) Grimes, R. N. *Carboranes*; Academic Press: New York, 1970.

(6) Williams, R. E. *Pure Appl. Chem.* **1972**, *29*, 569−583.

(7) Douglass, A. G.; Czuprynski, K.; Mierzwa, M.; Kaszynski, P. *Chem. Mater.* **1998**, *10*, 2399−2402 and references therein.

(8) (a) Hardy, G. E.; Callahan, K. P.; Strouse, C. E.; Hawthorne, M. F. *Acta Crystallogr.* **1976**, *B32*, 264−266. (b) Delaney, M. S.; Knobler, C. B.; Hawthorne, M. F. *Inorg. Chem.* **1981**, *20*, 1341−1347.

10.1021/ic991155e CCC: $19.00
Published on Web 07/01/2000

employment of computational methods for the investigation of these compounds may save time and expense.

Ab initio and semiempirical quantum chemical studies on boranes and carboranes have been reported many times. Such methods were successfully applied to the explanation and understanding of chemical bonding, and to the stability of polyhedral borane compounds, by Hoffmann and Lipscomb[10] (MO-LCAO calculations by the extended Hückel method), by King and Rouvray[11] (combination of graph theory and the Hückel method), by Aihara[12] (resonance energies), by Stone[13] (tensor surface harmonic theory), by Jemmis and Schleyer[14] (six interstitial electron rule), by Ott and Gimarc[15] (rule of topological charge stabilization), by Bader and Legare[16] (topology of charge density), and by Schleyer et al.[17] (nucleus independent chemical shifts). Other ab initio calculations have also been reported to investigate geometries, relative stabilities, and skeletal rearrangements.[18]

However, usage of high-level quantum chemical calculations for the investigation of molecular geometries of substituted borane and carborane cage compounds with large substituents, polymer chains, and/or molecular associations is still extremely time-consuming. For such purposes it might usually be better to use either MM methods or a combination of MM and ab initio methods.

Previously MM calculations were successfully used not only for the investigation of ordinary organic molecules but also for the modeling of the structures of such complicated molecules as π-complexes of metals,[19,20] metalloclasters,[21] and organometallic host−gest compounds.[22] As mentioned above, the extension of molecular mechanics calculations to the borane and carborane cage compounds has previously been successful. The problem of the description of a cage was solved by presenting a borane or carborane cage as a superposition of three (in the case of 7-vertex compounds) or four (in the case of 12-vertex compounds) formally independent fragments. Interactions between those fragments were described by the Hill-like potential usually used for the description of nonbonded interactions, and it was shown that such a description of the valence bonds is reasonable. The proposed approach has the distinct advantage in that it allows one to carry out conformational calculations within the standard MM3 program.[1]

Scheme 1

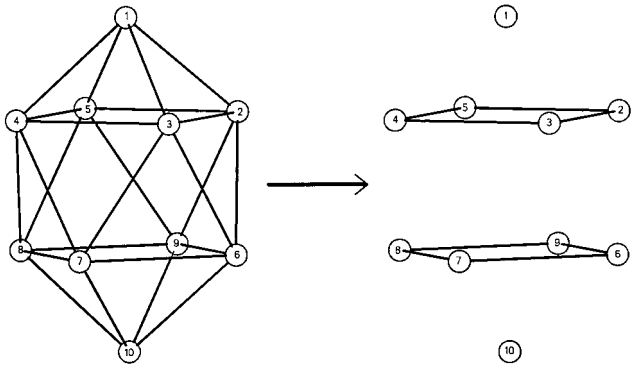

Other approaches for the description of intramolecular interactions when atoms (mostly metals) in the molecule have high coordination numbers have also been proposed. It is possible, for instance, to describe a metal−ligand (M−L) interaction using a dummy atom to represent such a symmetrical ligand as cyclopentadienyl or phenyl, thereby reducing the number of valence bonds and avoiding the description of a large number of X−M−Y bond angles (where X and Y are atoms of ligands).[19,20] In another approach, M−L interactions were described in terms of Coulomb-type potentials.[23]

In the present work we have continued modeling borane cage compounds in the same way as in our previous investigations.[2] This approach has been extended to the calculation of 10-vertex borane cage anions and molecules with the MM3(96) program.[1] The structures of the nonsubstituted $B_{10}H_{10}^{2-}$ anion and several substituted anions and molecules, investigated earlier by X-ray analysis, have been calculated to test our model.

Model and Parameter Set

It was shown[2] that the description of *n*-vertex borane cage molecules within the standard framework of the MM3 program leads to a very complicated situation. To use the MM3 program without any alterations, the 10-vertex borane cage has to be presented as a superposition of four formally independent "molecules" (two cap fragments and two ring fragments) (Scheme 1; atomic numbers are given according to the standard IUPAC numbering[24]).

Such a representation allowed us to avoid a description of all intracage valence bonds and angles, and to use only two types of boron atoms (cap boron and ring boron). Cap−ring and ring−ring interactions were described by Hill-like potentials

$$E_b = \frac{\epsilon_b}{D}\left[1.84 \times 10^5 \exp\left(\frac{-12.0R}{R_b}\right) - 2.25\frac{R^6}{R_b^6}\right]$$

where ϵ_b is close to the bond dissociation energy, R_b is an ideal valance bond distance, and D is the dielectric constant. The parameters ϵ_b and R_b of that potential were adjusted to reproduce the standard valence bonds. The success of the usage of such a potential for the description of valence bonds was shown for

(9) (a) Hawthorne, M. F. *Pure Appl. Chem.* **1991**, *63*, 327−334. (b) Hawthorne, M. F. *Angew. Chem., Int. Ed. Engl.* **1993**, *32*, 950−984. (c) Soloway, A. H.; Tjarks, W.; Barnum, B. A.; Rong, F.-G.; Barth, R. F.; Codogni, I. M.; Wilson, J. G. *Chem. Rev.* **1998**, *98*, 1515−1562.

(10) Hoffmann, R.; Lipscomb, W. N. *J. Chem. Phys.* **1962**, *36*, 2179−2189.

(11) King, R. B.; Rouvray, D. H. *J. Am. Chem. Soc.* **1977**, *99*, 7834−7840.

(12) Aihara, J. *J. Am. Chem. Soc.* **1978**, *100*, 3339−3342.

(13) (a) Stone, A. J. *Inorg. Chem.* **1981**, *20*, 563−571. (b) Stone, A. J.; Alderton, M. J. *Inorg. Chem.* **1982**, *21*, 2297−2302.

(14) (a) Jemmis, E. D. *J. Am. Chem. Soc.* **1982**, *104*, 7071−7020. (b) Jemmis, E. D.; Schleyer, P. v. R. *J. Am. Chem. Soc.* **1982**, *104*, 4781−4788.

(15) Ott, J. J.; Gimarc, B. M. *J. Am. Chem. Soc.* **1986**, *108*, 4303−4308.

(16) Bader, R. F. W.; Legare, D. A. *Can. J. Chem.* **1992**, *70*, 657−676.

(17) (a) Schleyer, P. v. R.; Najafian, K. *Inorg. Chem.* **1998**, *37*, 3454−3470. (b) Schleyer, P. v. R.; Subramanian, G.; Jiao, H.; Najafian, K.; Hofmann M. In *Advances in Boron Chemistry*; Siebert, W., Ed.; The Royal Society of Chemistry: Cambridge, England, 1997.

(18) See for example: (a) Ott, J. J.; Gimarc, B. M. *J. Comput. Chem.* **1986**, *7*, 673−692. (b) Buehl, M.; Schleyer, P. v. R. *J. Am. Chem. Soc.* **1992**, *114*, 477−491. (c) Mckee, M. L. *J. Am. Chem. Soc.* **1988**, *110*, 4208−4212; (d) Mckee, M. L. *J. Phys. Chem.* **1992**, *96*, 1679−1683. (e) Wales, D. J.; Stone, A. J. *Inorg. Chem.* **1987**, *26*, 3845−3850. (f) Wales, D. J. *J. Am. Chem. Soc.*, **1993**, *115*, 1557−1567. (g) Gimarc, B. M.; Ott, J. J. *J. Am. Chem. Soc.* **1987**, *109*, 1388−1392.

(19) (a) Timofeeva, T. V.; Lii, J.-H.; Allinger, N. L. *J. Am. Chem. Soc.* **1995**, *117*, 7452−7459. (b) Slovokhotov, Yu. L.; Timofeeva, T. V.; Sruchkov, Yu. T. *Z. Strukt. Khim. (Engl. Trans.)* **1987**, *28*, 463−471. (c) Timofeeva, T. V.; Slovokhotov, Yu. L.; Sruchkov, Yu. T. *Dokl. Akad. Nauk SSSR, Ser. Khim.* **1987**, *294*, 1173−1176.

(20) Doman, T. N.; Landis, C. R.; Bosnich, B. *J. Am. Chem. Soc.* **1992**, *114*, 7264−7272.

(21) Lauher, J. W. *J. Am. Chem. Soc.* **1986**, *108*, 1521−1531.

(22) Schneider, A. M.; Behrens, P. *Chem. Mater.* **1998**, *10*, 679−681.

(23) (a) Menger, F. M.; Sherrod, M. J. *J. Am. Chem. Soc.* **1988**, *110*, 8606−8611. (b) Thiem, H.-J.; Brandl, M.; Breslow, R. *J. Am. Chem. Soc.* **1988**, *110*, 8612−8616.

(24) Adams, R. M. *Pure Appl. Chem.* **1972**, *30*, 681−710.

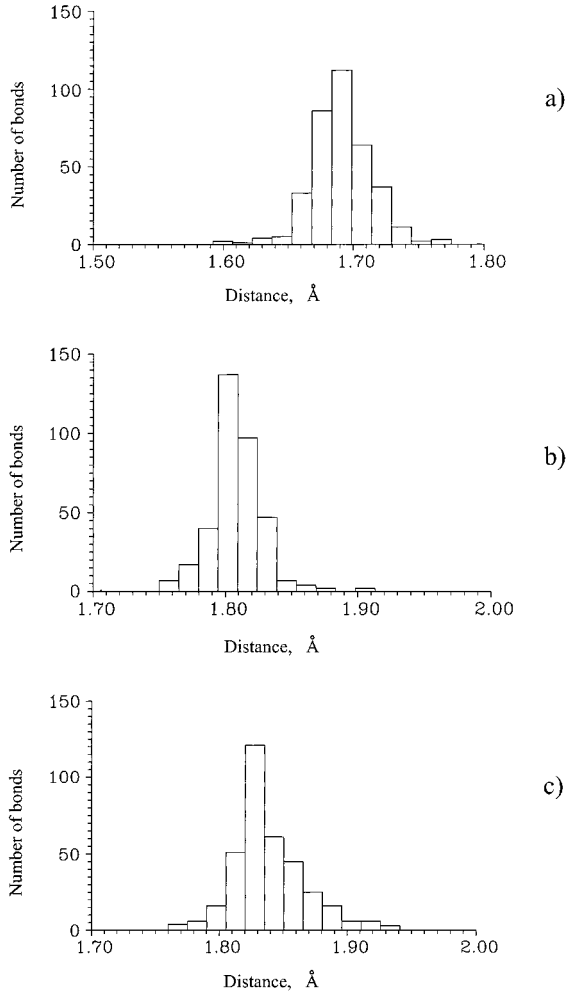

Figure 1. Histograms of the distribution of the bond lengths in 10-vertex boranes for different bond types: (a) cap−ring, (b) ring−ring, (c) intraring. The present distribution is obtained with the CSD program package V.5.14.[25] We took into consideration compounds with the following refcodes: BOVRAF, BUBCUW, DHBPCU, EAMBNO10, FIMMOD, FUDHIV, FUDHIV01, FUDHOB, FUDHOB02, FUZBUX, FUZVIF, HIFYEA, JAFGEC, KADMEH, KUMFIH, KUMFON, POCHOE, RACHIM, RACQAN, RAFYEC, RUHBOR, SORGEL, SORGIP, TEWTEU, TIZDUB, TOCLOM, TOCLUS, TOSYOP, VUKPEW, VUKPIA, WAKXIP, YAPXIW, YAPXIW10, YEDHUK, YEWSEY, YEYKOC, ZELZAR, ZELZEV, ZOXZUH.

the 7- and 12-vertex molecules.[2] We assume that it will be adequate for the description of the 10-vertex molecules and ions as well.

To find ideal values for the intracage bond lengths and bond angles, a statistical analysis of the structures of the 10-vertex boranes which were found in the Cambridge Structural Database (CSD) V.5.14[25] was carried out. It should be noted that parametrization in the MM3 program is mostly based on experimental data taken from the investigation of molecules in the gas phase. Strictly speaking, there is a difference in the treatment of the equilibrium bond lengths derived from different computational and experimental methods.[3a] However, this difference is usually very small (approximately 0.005 Å[3a]), and we will ignore this fact in the following text. During the analysis we took into account the symmetry of the isolated $B_{10}H_{10}^{2-}$ ion. There are three types of bonds in this cage: cap−ring, ring−ring, and intraring (see Scheme 1). Histograms of bond length distributions for each type are shown in Figure 1. We took into consideration all the compounds found, except for several (refcodes are FUYMIV, KUMFED, TMCPDB, VUJNAPO1) where the bond lengths of the same type were far away from the normal interval. For all other compounds (see refcodes in the caption to Figure 1) a wide range of bond lengths was found. It was not possible to explain these effects by the systematic influence of substituents. A similar situation took place when we were analyzing histograms for 12-vertex carboranes.[3c] We suppose that such a discrepancy for the same bond type might be caused by experimental errors in the bond length due to thermal motions of the borane cages. Nevertheless, all of the histograms exhibit a nearly Gaussian distribution. This fact allowed us to utilize the mean statistical values as the standard for bond lengths to find l_0 (ideal) values by adjusting the calculated values to the mean statistical ones. Intraring angles were found to be close to 90°, and this value was used as the ideal B−B−B bond angle.

The force constants were determined as follows. Our attempts to use published spectroscopic data to find force constants were unsuccessful. There are several publications devoted to the determination of the force constants for the borane and carborane cage compounds which have been reviewed by Leites.[26a] The correlations between force constants in the diverse parameter sets presented in that review[26b] appear to differ significantly in an unpredictable way.

Parameters for the intracage interactions such as B−B bonds, B−B−B and B−B−B−B bond and torsion angles, and B−H, B−B−H, B−B−B−H, and H−B−B−H bonds and angles were taken from our previous work.[2c] Exopolyhedral B−B−B−X torsion and B−B−X bond angles (here and in the following text of this section, the letters X, Y, and Z stand for the atoms of the substituents) were parametrized as B−B−B−H and B−B−H angles correspondingly. For B−B−X−Y angles, free rotation about the B−X bond was assumed. B−X−Y−Z torsion and B−X−Y bond angles were parametrized as for the corresponding C−X−Y−Z and C−X−Y angles. In the MM3 parameter set,[1] there are no force constants for B−X bonds where the boron atom is a cage atom. Therefore, the force constants for B−N, B−P, and B−S exopolyhedral bonds which appeared in the compounds under consideration were determined by ab initio calculations of the bond stretch energies using the GAUSSIAN94 program.[27] All calculations were carried out at the RHF/6-31G** level. As model compounds, $B_6H_5NO_2^{2-}$, $B_6H_5PH_3^{1-}$, and $B_6H_5SH_2^{1-}$ anions were utilized. For all these anions we have determined first the standard bond lengths by the geometry optimization, and after that, the interval of distances of $L_{stand} - 0.2$ to $L_{stand} + 0.2$ Å was scanned with a step of 0.1 Å. At each step, optimization of the geometry was carried out. The force constant needed in the MM3 bond stretch energy equation[1] to reproduce the energies was then determined by the least-squares procedure, so as to reproduce the distance/energy dependence obtained by ab initio calculation. This procedure was expected to give the force constants to within a few percent of their actual values. The TMS procedure will give stretching constants systematically high by 5−10%. The

(25) Allen, F. N.; Kennard, O. *Chem. Des. Auto. News* **1993**, *8*, 31−37.

(26) (a) Leites, L. A. *Chem. Rev.* **1992**, *92*, 279−323. (b) Table 16 in ref 26a.

(27) Frisch, M. J.; Trucks, G. W.; Schlegel, H. B.; Gill, P. M. W.; Johnson, B. G.; Robb, M. A.; Cheeseman, J. R.; Keith, T.; Petersson, G. A.; Montgomery, J. A.; Raghavachari, K.; Al-Laham, M. A.; Zakrzewski, V. G.; Ortiz, J. V.; Foresman, J. B.; Cioslowski, J.; Stefanov, B. B.; Nanayakkara, A.; Challacombe, M.; Peng, C. Y.; Ayala, P. Y.; Chen, W.; Wong, M. W.; Andres, J. L.; Replogle, E. S.; Gomperts, R.; Martin, R. L.; Fox D. J.; Binkley, J. S.; Defrees, D. J.; Baker, J.; Stewart, J. P.; Head-Gordon, M.; Gonzales, C.; Pople, J. A. *Gaussian 94*, Revizion E.2; Gaussian Inc.: Pittsburgh, PA, 1995.

Table 1. Stretching Parameters of the Ring and Cap Groups, L_0 (Å) and K_s (mdyn·Å^{-1})[a]

bond	L_0	K_s	bond	L_0	K_s
B(26)−B(26)	1.836	3.0	B(27)−H(5)	1.185	3.85
B(26)−H(5)	1.185	3.85	B(27)−N(46)	1.480	2.99
B(26)−P(25)	1.895	2.49	B(27)−N(45)	1.473	2.99
B(26)−N(110)	1.493	2.99	B(27)−S(16)	1.770	1.37
B(26)−O(41)	1.480	5.40	B(27)−B(27)	1.707	3.0

[a] In Tables 1−4, numbers in parentheses correspond to the atom types for the MM3 connectivity file. Type 26 is used for a ring boron atom, and type 27 is used for a cap boron atom. For other atoms, appropriate types from the MM3 program for the particular group were used.

Table 2. Parameters of the Ring−Ring, Ring−Cap (Valence Bonds), and Cap−Cap Interactions, R_b (Å) and ϵ_b (kcal·mol^{-1})

bond or nonbonded interaction	R_b	ϵ_b
B(26)−B(26)	1.803	35.0
B(27)−B(26)	1.678	20.0
B(27)···B(27)	2.35	0.01

Table 3. Bond Angle Bending and Out-of-Plane Parameters, θ_0 (Å) and K_θ (mdyn·Å^{-1})

angle	θ_0	K_θ	angle	θ_0	K_θ
B(26)−B(26)−B(26)	90.0	0.3	B(26)−O(41)−B(26)	115.0	0.95
H(5)−B(26)−B(26)	130.0	0.3	B(26)−O(41)−C(1)	118.0	1.0
O(7)−N(46)−B(27)	115.9	1.0	B(26)−O(41)−H(73)	116.0	0.85
B(27)−N(46)−B(27)	125.0	1.0	B(27)−H(5)−B(27)	110.0	0.2
N(10)−N(45)−B(27)	180.0	0.7	B(26)−B(26)−O(41)	130.0	0.3
C(1)−S(16)−B(27)	105.0	0.5	B(26)−B(26)		0.0
P(25)−B(26)−B(26)	130.0	0.3	B(26)−H(5)		0.0
B(26)−P(25)−P(50)	92.5	0.48	N(46)−B(27)		1.5
C(1)−P(25)−B(26)	95.6	0.77	B(26) −P(25)		0.0
B(26)−B(26)−N(110)	130.0	0.3	B(26)−N(110)		0.0
B(26)−N(110)−H(23)	116.7	0.70	N(110)−B(26)		0.0
B(26)−N(110)−C(2)	124.0	0.45	B(26)−O(41)		0.0

Table 4. Torsion Parameters (kcal·mol^{-1})

torsion angle	V_1	V_2	V_3
B(26)−B(26)−B(26)−B(26)	0.0	3.0	0.0
H(5)−B(26)−B(26)−H(5)	0.0	3.0	0.0
H(5)−B(26)−B(26)−B(26)	0.0	0.0	0.0
H(5)−C(1)−S(16)−B(27)	0.0	0.0	0.483
B(26)−B(26)−P(25)−C(1)	0.0	0.0	0.0
B(26)−B(26)−P(25)−C(50)	0.0	0.0	0.0
B(26)−B(26)−B(26)−P(25)	0.0	0.0	0.0
H(5)−B(26)−B(26)−P(25)	0.0	3.0	0.0
B(26)−P(25)−C(50)−C(50)	0.0	0.0	0.4
B(26)−P(25)−C(1)−H(5)	0.0	0.0	0.41
B(26)−B(26)−N(110)−H(23)	0.0	0.0	0.0
B(26)−B(26)−N(110)−H(2)	0.0	0.0	0.0
B(26)−B(26)−B(26)−N(110)	0.0	0.0	0.0
H(5)−B(26)−B(26)−N(110)	0.0	3.0	0.0
B(26)−N(110)−C(2)−O(6)	0.669	5.336	0.177
B(26)−N(110)−C(2)−C(2)	0.82	6.0	0.0
H(5)−B(26)−B(26)−O(41)	0.0	3.0	0.0
B(26)−B(26)−O(41)−B(26)	0.0	0.0	0.0
B(26)−B(26)−O(41)−C(1)	0.0	0.0	0.0
B(26)−B(26)−B(26)−O(41)	0.0	0.0	0.0
B(26)−B(26)−O(41)−H(73)	0.0	0.0	0.0
B(26)−O(41)−C(1)−C(1)	0.0	0.0	0.45
B(26)−O(41)−C(1)−H(5)	0.0	0.0	0.45

parameter set developed in the present work is listed in Tables 1−4. Some other parameters in those tables will be discussed in the following section.

We did not include electrostatic terms (bond dipoles) in the description of the borane cage. The reasons for that are as follows. Our previous investigations[2] showed that the molecular structures can be adequately described by nonbonded interaction and without explicitly taking into account electrostatics. The other reason comes from the quantum chemical investigations of borane anions and carboranes[2c] that showed that the polarity of the B−H bond is also almost equal to zero. As we will see below, only in a few cases is it necessary to involve the electrostatic term.

Table 5. Mean X-ray Bond Lengths for 10-Vertex Borane Anion $B_{10}H_{10}^{2-}$ Found in CSD, L_X,[25] MM3-Calculated, L_{MM3}, and ab Initio Calculated, $L_{q(1)}$ (RHF/STO-3G)[18a] and $L_{q(2)}$ (MP2(fc)/6-31G*)[17b] (Å)

bond type	L_X	L_{MM3}	$L_{q(1)}$	$L_{q(2)}$
cap−ring	1.690	1.690	1.673	1.702
ring−ring	1.809	1.809	1.795	1.814
intraring	1.838	1.838	1.826	1.832

Calculations

All molecular mechanics calculations were performed with the MM3(96) program.[1] It should also be noted that parameters for the nonbonded potential for boron−boron interactions in the MM3 program are dependent on the distance between two atoms. For distances longer than $1.2R_{vdw}$, normal nonbonded parameters are used, and for shorter distances (close to valence contacts), parameters developed in the previous section are utilized. Therefore, one should carefully choose the initial geometry.

Results and Discussion

Using the above-described approach, we have carried out calculations for the isolated $B_{10}H_{10}^{2-}$ (**I**) anion to adjust our results to the mean geometry characteristics found from the CSD. As has been underlined above, the isolated anion has three types of bonds. For the unsubstituted anion **I** we have obtained the same bond lengths and angles as the mean values found from the CSD. It was also interesting to compare these results with the results obtained by ab initio calculations[17b,18a] (Table 5). It can be seen that ab initio calculations exhibit the same trend in the bond length distribution.

For the evaluation of our approach, the structures of several substituted molecules and anions, which were previously investigated by the X-ray method, have been calculated, and their geometric characteristics have been compared. We have calculated the structures of several anions with small substituents to compare both their relative orientations and their intracage bond lengths. For other compounds, only relative orientations have been considered. It should be noted, however, that our approach does not take into account all of the details of the influence of the substituents on the intracage bond length distribution. Therefore, we were comparing only average values for each bond type, assuming that all the molecules and ions in question have the same symmetry as the isolated $B_{10}H_{10}^{2-}$ anion.

The calculation of 1-nitrononahydro-*closo*-decaborate(2−) (**II**) (Figure 2) showed that the mean values of bond lengths of the ring−ring and intraring types (L_{r-r} = 1.809 Å, L_{w-r} = 1.838 Å), as well as the orientation of the NO_2 group about the B−N bond (the projection of this group lies on the line connecting the centers of the B(2)−B(5) and B(3)−B(4) bonds, and the torsion angle B(2)−B(1)−N(1)−O(1) is equal to 45.0°), are in good agreement with experiment[29] (L_{r-r} = 1.803 Å, L_{w-r} = 1.831 Å, $\omega_{B(2)-B(1)-N(1)-O(1)}$ = 45.3°). However, experimental B(1)−B(n) (n = 2, 3, 4, 5) bond lengths appear to be shorter then calculated ones; the mean values are $L_{X\text{-ray}}$ = 1.670 Å and L_{MM3} = 1.692 Å. The same effect was observed for benzene substituted molecules with π-acceptor substituents, and in particular with the NO_2 group.[30] It was shown that the influence of π-acceptor substitution leads to the decrease of the nearest

(28) Takano, K.; Izuho, M.; Hosoya, H. *J. Phys. Chem.* **1992**, *96*, 6962−6969.
(29) Nachtigal, C.; Preetz, W. *Z. Anorg. Allg. Chem.* **1996**, *622*, 2057−2060.

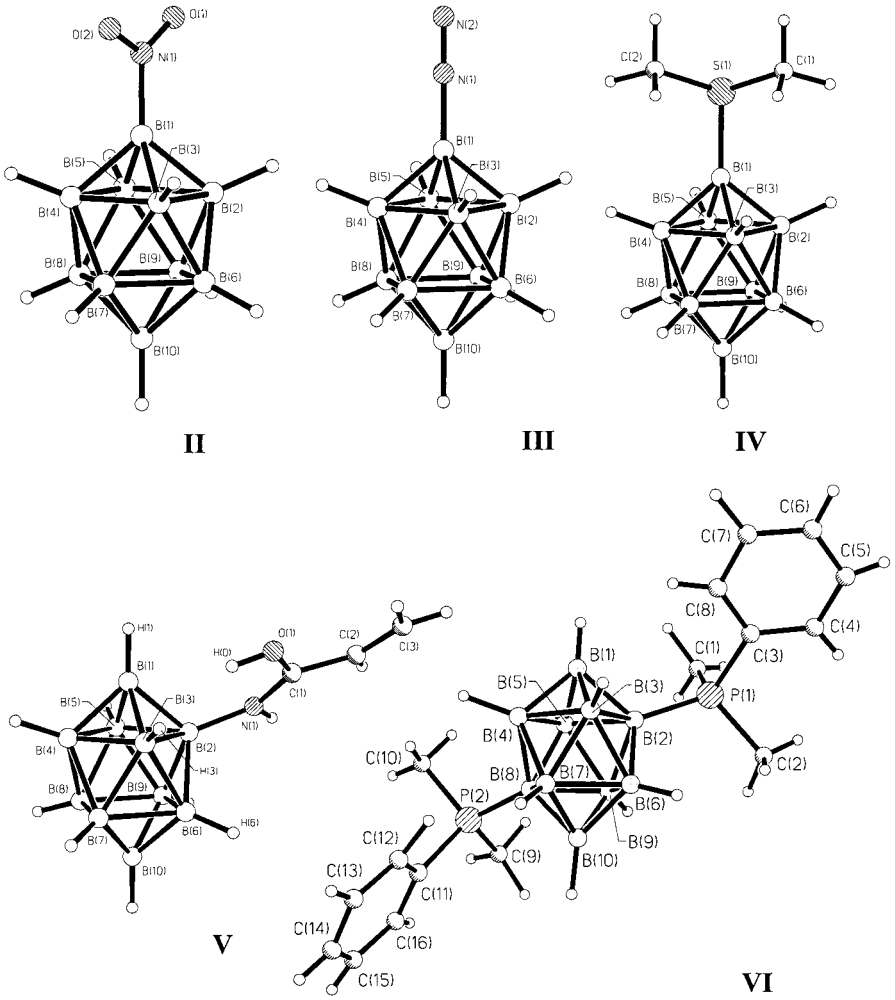

Figure 2. General view of one-cage compounds **II**−**VI**.

C−C bond lengths. Using the analogy between two-dimensional and three-dimensional aromatic systems, we assume that the decrease of the nearest B−B bond lengths is caused by the influence of the NO_2 group. As was mentioned above, the present approach does not take into account such effects. At the same time the mean experimental value of the B(10)−B(*n*) (*n* = 6, 7, 8, 9) bond lengths that are not directly influenced by the NO_2 group is very close to the calculated distance ($L_{X\text{-ray}}$ = 1.687 Å, L_{MM3} = 1.690 Å).

The same situation occurred when we compared the experimental[31] and calculated bond lengths for 1-azononahydro-*closo*-decaborate(1−) (**III**) (Figure 2), where the influence of the azo group leads to the decrease of the B(1)−B(*n*) (*n* = 2, 3, 4, 5) bond lengths ($L_{X\text{-ray}}$ = 1.656 Å, L_{MM3} = 1.690 Å). The mean value of the B(10)−B(*n*) (*n* = 6, 7, 8, 9) bonds appears to be almost the same as that from experiment ($L_{X\text{-ray}}$ = 1.687 Å, L_{MM3} = 1.690 Å). The mean experimental and calculated values of ring−ring bond lengths are in good agreement ($L_{X\text{-ray}}$ = 1.805 Å, L_{MM3} = 1.809 Å); however, the average experimental value for the intraring bond type appeared to be longer than the mean value derived from the statistical analysis, and therefore longer than the average MM3 value ($L_{X\text{-ray}}$ = 1.853 Å, L_{MM3} = 1.837 Å).

Table 6. Comparison of Calculated and X-ray[32] Geometry Characteristics for Anion IV (Distances, Å; Angles, deg)

geometry characteristic	MM3	X-ray	
		anion **IVa**	anion **IVb**
cap−ring type	1.692	1.708	1.726
intraring type	1.837	1.862	1.871
ring−ring type	1.810	1.828	1.809
C(1)−S(1)−C(2)	98.2	99.4	103.4
B(1)−S(1)−C(1)	107.4	105.5	104.7
B(1)−S(1)−C(2)	107.5	106.2	104.3
B(3)−B(1)−S(1)−C(1)	35.3	34.9	100.7
B(3)−B(1)−S(1)−C(2)	−69.5	−70.0	−7.6

Calculated and experimental[32] geometric characteristics for the 1-(dimethyl sulfide)nonahydro-*closo*-decaborate(1−) (**IV**) (Figure 2) are compared in Table 6. The unit cell of the crystal contains two symmetrically independent anions (**IVa** and **IVb**). For anion **IVa**, we obtained a good reproduction of the orientation of the SMe_2 group relative to the borane cage. However, the orientation of this group in anion **IVb** of the crystal differs from its orientation in **IVa**, and from the calculated results. We suppose that the orientation of the substituent SMe_2 in this case is influenced by the cation $Pb(2,2'\text{-BiPy})_2^{2+}$. Contacts between the S atom in **IVb** and several atoms of $Pb(2,2'\text{-BiPy})_2^{2+}$ (Figure 3) are close to the sum of the crystallographic van der Waals radii of these atomic pairs (see the caption to Figure 3).

(30) Domenicano, A. In *Accurate Molecular Structures: Their Determination and Importance*; Domenicano, A., Hargittai, I., Eds.; Oxford University Press: Oxford, New York, 1992.

(31) Ng, L.-L.; Ng, B. K.; Shelly, K.; Knobler, C. B.; Hawthorne, M. F. *Inorg. Chem.* **1991**, *30*, 4278−4280.

(32) Orlova, A. M.; Sivaev, I. B.; Lagun, V. L.; Katser, S. B.; Solntsev, K. A.; Kuznetsov, N. T. *Koord. Khim.* **1993**, *19*, 116−121.

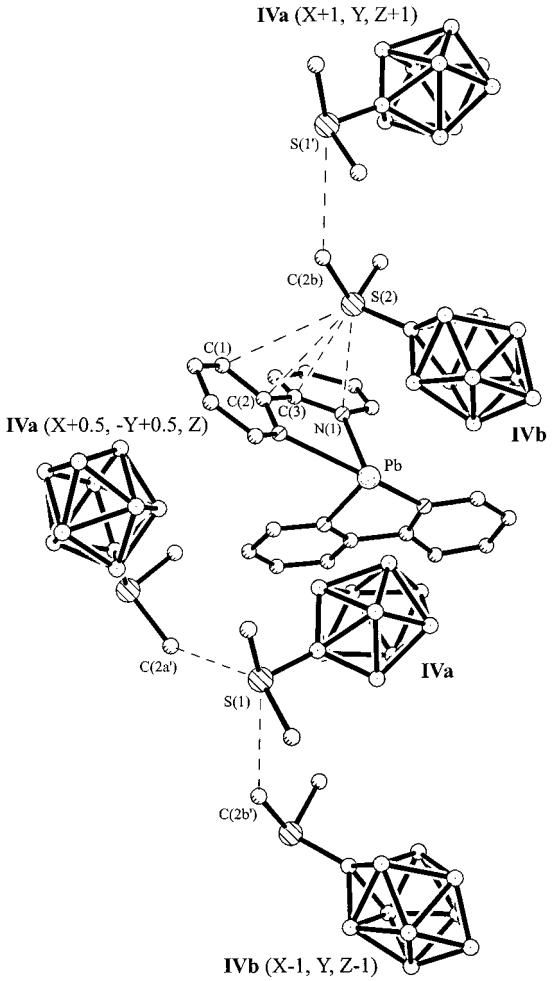

Figure 3. Fragment with crystal packing of $Pb(2,2'\text{-}BiPy)_2(1\text{-}B_{10}H_9S\text{-}(CH_3)_2)_2$. Only the necessary atomic numbers are given. Interatomic contacts in question are shown with dashed lines. Selected interatomic distances are S(1)−C(2b′) = 3.754 Å, S(1)−C(2a′) = 3.526 Å, S(2)−C(1) = 3.756 Å, S(2)−C(2) = 3.444 Å, S(2)−C(3) = 3.511 Å, S(2)−N(1) = 3.513 Å, S(1′)−C(2b) = 3.754 Å.

This restricts the rotation of the substituent and leads to the discrepancy between calculated and experimental data. On the other hand, there is no such restriction on the rotation of the SMe_2 group in **IVa**, and its orientation is mostly defined by intramolecular interactions. All of the experimental intracage bond lengths except for the ring−ring type of the **IVb** anion appear to be much longer than the calculated ones, and a wide range of the bond length distribution of the same bond type was found in the experiment.

The relative orientation of the NH═C(OH)−CH═CH_2 substituent in 2-(acrylamido)nonahydro-*closo*-decaborate(1−) (**V**) (Figure 2) has been investigated. We have estimated parameters for the C−N−C−O torsion angle using ab initio calculations at the RHF/6-31G** level, because they are missing in the MM3 parameter set.[1] These parameters were used for the description of the exopolyhedral B−N−C−O torsion angle as discussed in the previous section. The cation $H_3C{-}N^+H{=}C(OH){-}CH{=}CH_2$ was utilized as a model compound. Rotation about the N═C bond was carried out with a step size of 15°. Torsion parameters were determined by fitting the MM3 energy/angle curve to the ab initio one. Both curves are depicted in Figure 4, and the parameters are listed in Table 4.

Using the parameters developed, rotation of the substituent about the B(2)−N(1) bond with a step size of 15° (rotation angle ω = B(3)−B(2)−N(1)−C(1)) was carried out to investigate

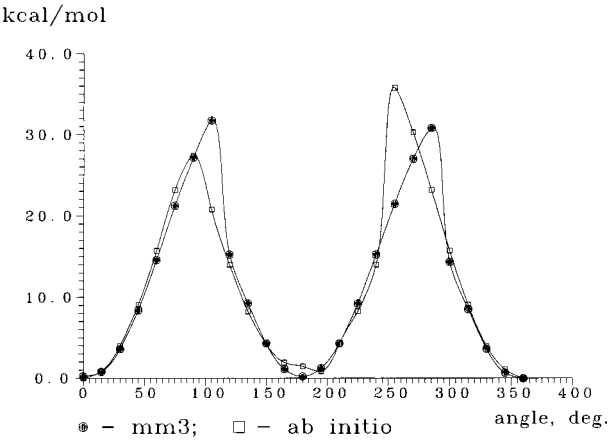

Figure 4. Ab initio and MM3 torsion curves for C−N═C−O angle in anion **V**.

Table 7. Comparison of Calculated and X-ray[33] Geometry Characteristics for Anion V (Distances, Å; Angles, deg)

geometry characteristic	MM3		ab initio	
	$\omega = 30°$	$\omega = -14.5°$	RHF/6-31G**	X-ray
B(2)−N(1)	1.523	1.519	1.556	1.522
H(O)···B(1)		2.717	2.482	2.438
H(O)···B(2)	2.588	2.593	2.403	2.325
H(O)···B(3)	2.584	2.559	2.300	2.262
H(O)···B(6)	2.706			
H(O)···H(1)		2.743	2.523	2.466
H(O)···H(3)	2.366	2.301	2.065	2.038
H(O)···H(6)	2.490			
B(1)−N(1)−C(1)	129.1	129.1	126.6	125.6
B(3)−B(2)−N(1)−C(1)	30.0	−14.5	−14.5	−14.5
B(2)−N(1)−C(1)−O(1)	−0.4	−1.7	−3.6	−6.0
N(1)−C(1)−O(1)−H(O)	−0.6	−8.4	−0.7	0.5

the relative orientation of the $NHC(OH)C_2H_3$ in the isolated anion **V**. Only the symmetry-independent part with respect to the plane B(2)−B(4)−X−Y (X and Y are the center points of the B(7)−B(8) and B(6)−B(9) bonds, respectively) was taken into consideration. The minimum of the conformational energy occurs at a torsion angle of 30°. Selected geometric characteristics for this conformer are presented in Table 7.

The value of the B(3)−B(2)−N(1)−C(1) angle for the experimental structure[33] is equal to −14.5°, and significantly differs from the result of our calculation. In the experimental structure the hydroxyl H(O) atom is located above the B(1)−B(2)−B(3) triangle face, and some close H···B and H···H contacts are observed. The location of the same hydrogen in the calculated structure is above the other B(3)−B(2)−B(6) face, and all of the H···B and H···H contacts are longer than those in the experimental structure (Table 7). It is also interesting to consider the calculated conformer with a B(3)−B(2)−N(1)−C(1) torsion angle of −14.5°. The energy difference between the two calculated conformers is very small, 0.25 kcal·mol^{-1}. It can be seen from Table 7 (third column) that the H(O) atom appears to be more twisted out of the plane in comparison with the experimental data. To better understand this situation, an ab initio calculation of **V** at RHF/6-31G** was carried out. We optimized the geometry from the X-ray structure as a starting point, without symmetry constraints. However, the optimization procedure led to C_s symmetry (the symmetry plane was described above). We have also carried out another calculation fixing the torsion angle B(3)−B(2)−N(1)−C(1) in accord with the experimental value of −14.5°. The difference in the energies of these conformations was found to be small, 0.65 kcal·mol^{-1}.

(33) Siriwardane, U.; Chu, S. S. C.; Hosmane, N. S.; Zhang, G.; Zhu, W.; Zhu, H. *Acta Crystallogr.* **1989**, *C45*, 294−297.

Table 8. Comparison of Calculated and X-ray[34] Geometry Characteristics for Molecule VI (Distances, Å; Angles, deg)

geometry characteristic	MM3	X-ray	geometry characteristic	MM3	X-ray
B(2)−P(1)	1.895	1.900	B(3)−B(2)−P(1)−C(1)	−140.9	−132.2
B(8)−P(2)	1.895	1.886	B(4)−B(3)−B(2)−P(1)	146.1	150.5
B(2)−P(1)−C(3)	109.6	114.8	B(7)−B(8)−P(2)−C(11)	−13.9	−16.7
B(8)−P(2)−C(11)	110.3	113.1	B(7)−B(8)−P(2)−C(9)	−140.6	−139.4
B(3)−B(2)−P(1)−C(3)	−14.9	−13.5	B(7)−B(8)−P(2)−C(10)	108.0	102.4
B(3)−B(2)−P(1)−C(2)	107.8	108.3	B(6)−B(7)−B(8)−P(2)	146.3	152.0

Table 9. Comparison of Calculated and X-ray[35] Geometry Characteristics for Anion VII (Distances, Å; Angles, deg)

geometry characteristic	MM3	X-ray	geometry characteristic	MM3	X-ray
H(9)···H(19)	2.697	2.467	B(10)−N(1)−B(20)	125.9	125.7
H(6)···H(18)	2.722	2.420	B(10)−N(1)−O(1)	117.1	116.3
B(10)···B(20)	2.666	2.641	B(20)−N(1)−O(1)	117.1	117.9
			B(9)−B(10)···B(20)−B(19)	28.9	11.0

Selected geometric characteristics of the optimized anion **V** with a fixed torsion angle are listed in Table 7. It can be seen that good agreement between calculated and experimental values was found. The H(O) atom is located in the plane of the substituent and above the B(1)−B(2)−B(3) triangle face. Such a location is most probably stabilized by both conjugation with the π-system of the N═C−C═C fragment as outlined in ref 33 and electrostatic interactions of H(O) ($q_{H(O)} = +0.43$) to the closest atoms of the borane cage ($q_{B(1)} = +0.01$, $q_{B(2)} = +0.07$, $q_{B(3)} = -0.09$, $q_{H(1)} = -0.10$, $q_{H(3)} = -0.12$). The charge distribution in **V** was obtained from the HF/6-31G** wave function using the Mulliken population analysis incorporated in GAUSSIAN94. Now we can explain the difference between the location of the hydrogen atom derived from the MM3 calculation and that found experimentally. It arises from the fact that our model does not take into consideration all the details of charge distribution. Contacts between the H(O) atom and the closest boron and hydrogen atoms are too short to be reproduced by the nonbonded MM potential. Repulsion between the H(O) and the cage atoms leads to displacement of the hydrogen atom out of the plane. That in turn increases the N(1)−C(1)−O(1)−H(O) torsion energy, thereby increasing the total energy of this conformer.

The calculation of the 2,8-bis(dimethylphenylphosphine)-*closo*-decaborane (**VI**) (Figure 2) was carried out to investigate the relative orientation of the $PPhMe_2$ substituents and the borane cage. Since these two substituents do not appear to interact, we rotated one of them about the B(2)−P(1) bond with the step size of 15° (rotational angle ω = B(3)−B(2)−P(1)−C(3)). The data obtained demonstrated that the rotation barrier is small, 0.6 kcal·mol^{-1}, and the differences between the energies at the minima (less than 0.1 kcal·mol^{-1}) are not larger than the error of the method. The structure corresponding to the calculated global minimum ($\omega = -15°$) is the closest to the experimental geometry.[34] Using this structure as the initial geometry, we then optimized the geometry to obtain the molecular structure without any torsion angle restriction. The calculated and experimental geometry parameters, which define the relative orientation of the substituents, are listed in Table 8. The results obtained show almost the same molecular structure as that from experiment. This allows us to conclude that the geometry of **VI** in a crystal is mostly defined by intramolecular interactions.

We have also calculated the structures of several anions containing two boron cages to investigate and compare their relative orientations (Figure 5).

The calculated and experimental[35] geometries for μ-nitroso-(nonahydrodecaborate)(3−) (**VII**) (Figure 5) are compared in Table 9. To describe the relative orientation of the two borane cages, B(9)−B(10)···B(20)−B(19), a pseudotorsion angle was chosen. It can be seen from Table 9 that calculated values of both the pseudotorsion angle and the H···H contacts are larger than those from experiment. It should be noted that the standard H···H equilibrium nonbonded distance in the MM3 program (3.24 Å) is significantly larger than the standard crystallographic non-bonded H···H contact (2.4 Å) (for details, see ref 2a). This fact leads to the increase of the calculated B(9)−B(10)···B(20)−B(19) pseudotorsion angle in comparison with the experimental value to keep H···H distances closer to the MM3 equilibrium value. The other characteristics such as angles at the N atom and B(10)···B(20) distance are in good agreement with experiment.

The X-ray investigation of the structure of the $B_{20}H_{18}^{4-}$ anion (**VIII**), where two borane cages are joined by an apical−apical B−B bond,[36] has shown that the relative orientation of the two borane cages corresponds to an eclipsed conformation (Figure 5). Our calculation shows that the energies of eclipsed and staggered conformations appear to be the same. This fact allows us to assume that the structure of **VIII** in the crystal is not restricted by intramolecular interactions that lead to a centrosymmetric geometry according to the principle[37] that symmetric molecules placed in a crystal try to retain their inversion center rather than their other symmetry elements.

The structures of $[\mu\text{-}B_{20}H_{17}R]^{2-}$ anions (R = OH (**IX**), $O(CH_2)_4O(CH_2)_2CH(CH_3)_2$ (**X**)) have been investigated by the X-ray method, and the deprotonation of **X**, resulting in the formation of $[\mu\text{-}B_{20}H_{16}O(CH_2)_4O(CH_2)_2CH(CH_3)_2]^{3-}$ (**XI**, has been shown.[38] These compounds have been studied due to their potential application in the boron neutron capture therapy of tumors. Anions **IX** and **X** represent species where two borane cages are joined by bridge hydrogen and oxygen atoms (Figure 5). As was found by X-ray investigations,[38] the six-membered B−B−O−B−B−H rings in structures **IX** and **X** are planar. We have compared the MM results for these compounds with experiment. The bond angle at the H(bridge) atom was parametrized with a weak bending force constant (Table 3). The bridge oxygen atom was described in the same way as the furan oxygen, with slightly increased bond angles because the angles in a six-membered ring are larger than those in a five-membered ring (Tables 1−4). In Table 10, selected calculated geometric

(34) Jasper, S. A. Jr.; Jones, R. B.; Mattern, J.; Huffman, J. C.; Todd, L. J. *Inorg. Chem.* **1994**, *33*, 5620−5624.

(35) Schwalbe, C. H.; Lipscomb, W. N. *Inorg. Chem.* **1971**, *10*, 160−170.

(36) Ng, L.; Ng, B. K.; Knobler, C. B.; Hawthorne, M. F. *Inorg. Chem.* **1992**, *31*, 3669−3671.

(37) Kitaigorodskii, A. I. *Organic Chemical Crystallography*; Consultants Bureau: New York, 1961.

(38) (a) Li, F.; Shelly, K.; Kane, R. R.; Knobler, C. B.; Hawthorne, M. F. *J. Am. Chem. Soc.* **1996**, *118*, 6506−6507. (b) Li, F.; Shelley, K.; Kane, R. R.; Knobler, C. B.; Hawthorne, M. F. *Angew. Chem., Int. Ed. Engl.* **1996**, *35*, 2646−2649.

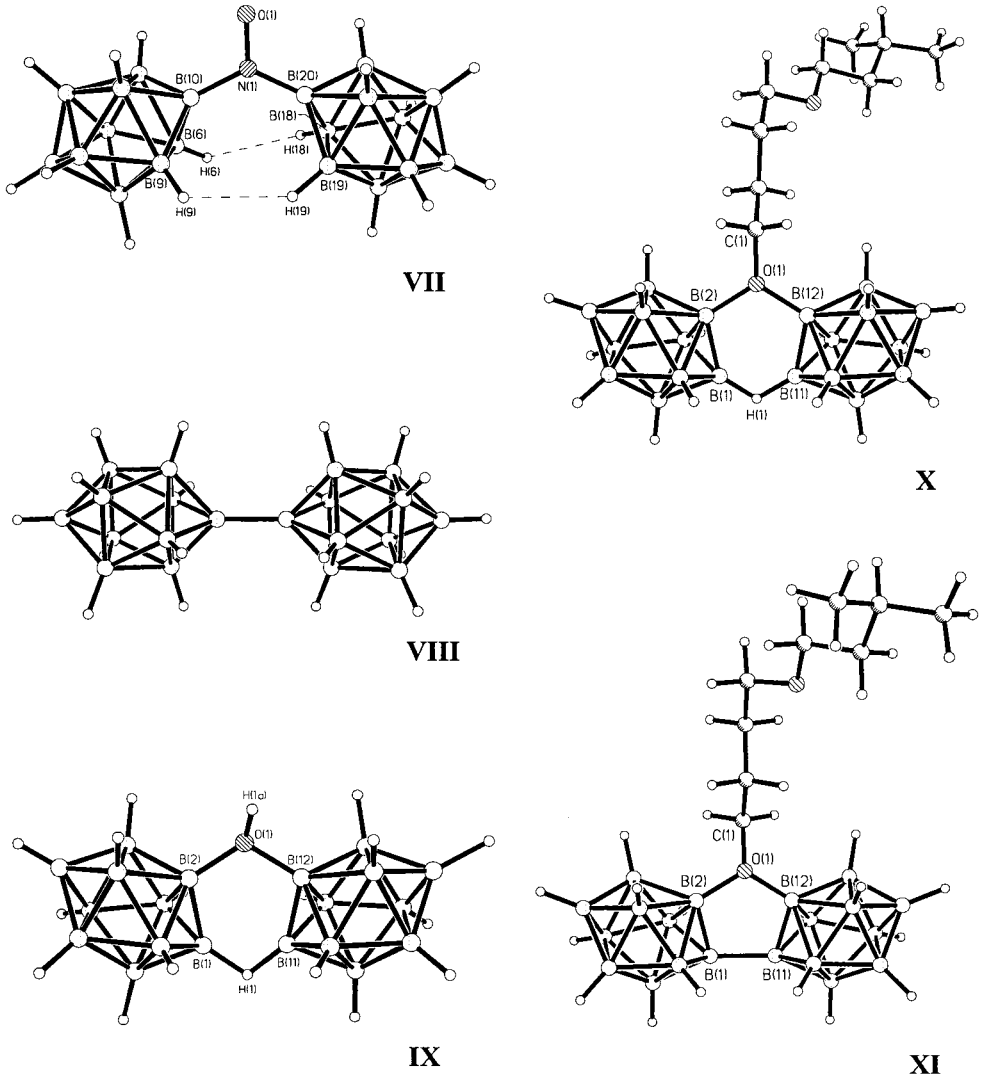

Figure 5. General view of two-cage compounds **VII**−**XI**. Only the necessary atomic numbers are given. Closest H···H contacts in anion **VII** are shown with dashes lines.

Table 10. MM3 Calculated and X-ray[38] Geometry Characteristics for Anions **VIII** and **IX** and MM3-calculated Geometry Characteristics for Anion X (Distances, Å; Angles, deg)

	anion **VIII**		anion **IX**		anion **X**
geometry characteristic	MM3	X-ray	MM3	X-ray	MM3
O(1)−B(2)	1.488	1.472	1.494	1.500	1.496
O(1)−B(12)	1.488	1.492	1.494	1.499	1.496
B(1)···B(11)	1.943	1.908	1.934	1.894	1.714
B(2)−O(1)−B(12)	113.9	114.5	114.7	113.4	112.8
B(1)−H(1)−B(11)	108.9	104.3	108.2	112.3	
B(2)−B(1)−B(11)−B(12)	−0.0	−0.7	−1.1	0.0	0.1
B(1)−B(11)−B(12)−O(1)	−0.1	−3.7	−4.0	−1.5	1.7
B(11)−B(12)−O(1)−C(1)			145.2	173.7	127.5
B(11)−B(12)−O(1)−H(1a)	139.1	161.7			

characteristics are compared with experimental results.[38] The MM3 calculations and X-ray data are in good agreement except for the position of H(1a) in **IX** and C(1) in **X**. The deviations of these atoms out of the planes of the six-membered ring are larger than those in the experimental structures. However, it can be seen that the geometry of **X** is characterized by a B(11)−B(12)−O(1)−C(1) torsion angle which is closer to 180° than B(11)−B(12)−O(1)−H(1a) in **IX** (Table 10). Our computational results demonstrate the same trend.

On the basis of the agreement of the previous two calculations with experiment, we have calculated the unknown structure of **XI** that seems to be close to the structure of **X** (Figure 5). In this case, the oxygen atom was parametrized as furan oxygen.[3] Selected geometric characteristics are listed in Table 10. The five-membered B−B−O−B−B ring also appeared to be planar. The B(2)−O(1)−B(12) bond angle is smaller than that for **X**, and the position of the C(1) atom is moved slightly out of the plane.

This work shows that the molecular mechanics calculations in general give reasonable molecular geometries. The speculation that the relative orientations of substituents and borane cages are mostly defined by intramolecular nonbonded interactions is confirmed by the good agreement between the calculated (gas-phase) and experimental (crystal-phase) results. Such calculations can be useful not only for the investigations of the molecular structures of substituted borane cage molecules, but also for the modeling of molecular packing in a crystal.

Acknowledgment. We thank Dr. Carolyn B. Knobler for providing us with the experimental molecular geometries prior to publication and for interesting and useful discussion and Mr. David Thornburg for help during the manuscript preparation. We also thank Dr. Jenn-Huei Lii for help with the MM3 program. The present work was supported by the U.S. Civilian Research and Development Foundation (CRDF), Grant RC2-147.

IC991155E